Electric Dipole Tensor Scattering from a Finitely Conducting Cylinder

Allen Q. Howard, Jr. ,
INSTITUTO DE GEOCIÊNCIAS,
PROGRAMA DE PÓS-GRADUAÇÃO EM GEOFÍSICA, Universidade do Pará

Abstract

This paper presents a summary of a time harmonic analysis of vector electromagnetic scattering from a finite conducting circular cylinder for an arbitrarily oriented electric dipole source. The method uses the classical separation of variables method with a Fourier series angular mode series and a Fourier integral representation over axial wave numbers. Several numerical checks are made to validate the resulting numerical algorithms for both incident and total fields for all six complex electromagnetic field components and for all three independent source polarizations.

Introduction

The classical problem of electromagnetic scattering from a finite conducting cylinder for an arbitrarily oriented electric dipole has been studied by many authors. Papas (Papas, 1950) gave the scalar solution for a line source parallel to the cylinder axis and determines both low and high frequency limits. Wait in his book *Scattering from Cylindrical Structures* considers vector axial dipole scattering from a circular wedge region (Wait, 1959). The three-dimensional scattering case for an axial oriented electric dipole is also known (Tsandoulas,1968). In his book on dyadic Green's functions C.T. Tai (Tai, 1971) formulates the dielectric cylinder scattering problem for an arbitrary source dyad. The results however are not complete for computation. A more recent work (Hongo, 2008) derives the general expressions for perfectly conducting and impedance boundary conditions for the electromagnetic field in cylindrical coordinates for an arbitrary oriented electric dipole. The purpose here is to derive, code and numerically evaluate the yet more general case of the classical separation of variables technique for a finite conducting cylinder illuminated by an arbitrarily oriented electric dipole. It seems surprising that this result is evidentially not generally available in the literature. In this era of general 3D numerical electromagnetic solvers the result is perhaps no longer important computationally except as a check on more general numerical methods. The motivation here is to validate the accuracy of our finite-difference frequency-domain electromagnetic solver.

Theory

The formulation of electromagnetic fields in cylindrical geometry for axi-symmetric scatters is simplified by using the axial components $(\mathrm{E}_z, \mathrm{H}_z)$ as potentials. For example, this is common practice in the analysis of fiber optical waveguides (Okamoto, 2006). The cylindrical geometry of the problem prompts using a Fourier representation for a generic component $\mathrm{A}(\rho,\phi,z)$ of the form

$$\mathrm{A}(\rho,\phi,z) = \sum_{n=-\infty}^{\infty} e^{in\phi} \int_{-\infty}^{\infty} \tilde{\mathrm{A}}_n(K,\rho) e^{iKz} \frac{\mathrm{d}K}{2\pi} . \qquad (1)$$

It is convenient to represent the electric dipole fields in cylindrical coordinates using axial components $\mathrm{E}_z(\rho,\phi,z)$ and $\mathrm{H}_z(\rho,\phi,z)$. A time harmonic factor of $e^{-i\omega t}$ is assumed and suppressed. The magnetic permeability is assumed constant and equal to the vacuum value $\mu_0 = 4\pi 10^{-7}$ [H/m]. The six curl Maxwell equations are solved for the ϕ and ρ components in terms of the source and z field components to obtain

$$\begin{aligned}
\tilde{\mathrm{E}}_{n\phi} &= \tfrac{1}{\gamma^2}\left[-i\omega\mu_0(\tfrac{\partial \tilde{\mathrm{H}}_{nz}}{\partial\rho} + \tilde{\mathrm{J}}_{n\phi}) - \tfrac{nK}{\rho}\tilde{\mathrm{E}}_{nz}\right], \\
\tilde{\mathrm{E}}_{n\rho} &= \tfrac{1}{\gamma^2}\left[i\omega\mu_0(\tfrac{in}{\rho}\tilde{\mathrm{H}}_{nz} - \tilde{\mathrm{J}}_{n\rho}) + iK\tfrac{\partial \tilde{\mathrm{E}}_{nz}}{\partial\rho}\right]. \\
\tilde{\mathrm{H}}_{n\phi} &= \tfrac{-1}{\gamma^2}\left[iK(\tfrac{-in}{\rho}\tilde{\mathrm{H}}_{nz} + \tilde{\mathrm{J}}_{n\rho}) + \tilde{\sigma}\tfrac{\partial \tilde{\mathrm{E}}_{nz}}{\partial\rho}\right], \\
\tilde{\mathrm{H}}_{n\rho} &= \tfrac{1}{\gamma^2}\left[iK(\tfrac{\partial \tilde{\mathrm{H}}_{nz}}{\partial\rho} + \tilde{\mathrm{J}}_{n\phi}) + \tfrac{in\tilde{\sigma}}{\rho}\tilde{\mathrm{E}}_{nz}\right].
\end{aligned} \qquad (2)$$

where the associated axial fields are

$$\begin{aligned}
& w\tfrac{\mathrm{d}}{\mathrm{d}w}\left(w\tfrac{\mathrm{d}\tilde{\mathrm{E}}_{nz}}{\mathrm{d}w}\right) + (w^2 - n^2)\tilde{\mathrm{E}}_{nz} \\
&= \tfrac{-1}{\tilde{\sigma}}\left[w^2\tilde{\mathrm{J}}_{nz} + \tfrac{iKw}{\gamma}\tfrac{\mathrm{d}}{\mathrm{d}w}(w\tilde{\mathrm{J}}_{n\rho}) - \tfrac{nKw}{\gamma}\tilde{\mathrm{J}}_{n\phi}\right], \\
& w\tfrac{\mathrm{d}}{\mathrm{d}w}\left(w\tfrac{\mathrm{d}\tilde{\mathrm{H}}_{nz}}{\mathrm{d}w}\right) + (w^2 - n^2)\tilde{\mathrm{H}}_{nz} \\
&= \tfrac{-w}{\tilde{\sigma}}\left[\tfrac{\mathrm{d}}{\mathrm{d}w}(w\tilde{\mathrm{J}}_{n\phi}) - in\tilde{\mathrm{J}}_{n\rho}\right]. - \tfrac{nKw}{\gamma}\tilde{\mathrm{J}}_{n\phi}\Big].
\end{aligned} \qquad (3)$$

Note the left hand sides of the two ordinary second order differential equations in (3) are solutions to Bessel's equation of order n for the independent unit-less radial variable $w = \gamma\rho$. The right hand sides are the known dipole source currents. Here $\gamma = (k^2 - K^2)^{1/2}$ and $\mathrm{Im}(\gamma) \geq 0$. The solution of equation (3) for a z directed dipole is

$$\begin{aligned}
\tilde{\mathrm{E}}^{(0,z)}_{nz} &= \tfrac{-\omega\mu_0\gamma^2}{4k^2} I_0 \mathrm{d}\ell e^{-in\phi_T} e^{-iKz_T} J_n(\gamma\rho_<) H^{(1)}_n(\gamma\rho_>), \\
\tilde{\mathrm{H}}^{(0,z)}_{nz} &= 0 .
\end{aligned} \qquad (4)$$

The remaining source polarizations are more difficult to evaluate because they involve the derivative of the Dirac delta function. The derivatives are interpreted by integration by parts, i.e., for $\varepsilon > 0$ and assuming $f(x')$ is continuous at $x' = x$,

$$\int_{x-\varepsilon}^{x+\varepsilon} f(x')\,\delta'(x')\,\mathrm{d}x' = -f(x)\,. \tag{5}$$

For ϕ directed dipoles we find

$$\begin{aligned}
\tilde{\mathrm{E}}_{nz}^{(0,\phi)} &= \tfrac{\omega\mu_0 n\ K}{4k^2\rho_T} I_0 \mathrm{d}\ell e^{-in\phi_T} e^{-iKz_T} J_n(\gamma\rho_<)\, H_n^{(1)}(\gamma\rho_>)\,, \\
\tilde{\mathrm{H}}_{nz}^{(0,\phi)} &= \tfrac{-i\gamma}{4} I_0 \mathrm{d}\ell\, e^{-in\phi_T} e^{-iKz_T} J_n(\gamma\rho_<)\, H_n^{(1)\prime}(\gamma\rho_>)\,, \rho < \rho_T\,, \\
&= \tfrac{-i\gamma}{4} I_0 \mathrm{d}\ell e^{-in\phi_T} e^{-iKz_T} J_n'(\gamma\rho_<)\, H_n^{(1)}(\gamma\rho_>)\,, \rho > \rho_T\,,
\end{aligned} \tag{6}$$

and similarily the ρ-directed dipole results are

$$\begin{aligned}
\tilde{\mathrm{E}}_{nz}^{(0,\rho)} &= \tfrac{i\omega\mu_0 K\gamma}{4k^2} I_0 \mathrm{d}\ell e^{-in\phi_T} e^{-iKz_T} J_n(\gamma\rho_<)\, H_n^{(1)\prime}(\gamma\rho_>)\,, \rho < \rho_T\,, \\
&= \tfrac{i\omega\mu_0 K\gamma}{4k^2} I_0 \mathrm{d}\ell e^{-in\phi_T} e^{-iKz_T} J_n{}'(\gamma\rho_<)\, H_n^{(1)}(\gamma\rho_>)\,, \rho > \rho_T\,, \\
\tilde{\mathrm{H}}_{nz}^{(0,\rho)} &= \tfrac{n}{4\rho_T} I_0 \mathrm{d}\ell\, e^{-in\phi_T} e^{-iKz_T} J_n(\gamma\rho_<)\, H_n^{(1)}(\gamma\rho_>)\,.
\end{aligned} \tag{7}$$

Given source fields $\tilde{\mathscr{E}}_{nz}^{(0,q)}, \tilde{\mathscr{H}}_{nz}^{(0,q)}$ where

$$\begin{aligned}
\tilde{\mathrm{E}}_{nz}^{(0,q)} &= \mathscr{E}_{nz}^{(0,q)} J_n(\gamma_2 a)\,, \\
\tilde{\mathrm{H}}_{nz}^{(0,q)} &= \mathscr{H}_{nz}^{(0,q)} J_n(\gamma_2 a)\,,
\end{aligned} \tag{8}$$

and where $q = \rho, \phi, z$ designates source orientation, we solve for the 4 unknown amplitudes $\tilde{\mathscr{E}}_{nz}^{(i,q)}, \tilde{\mathscr{H}}_{nz}^{(i,q)}, \tilde{\mathscr{E}}_{nz}^{(s,q)}, \tilde{\mathscr{H}}_{nz}^{(s,q)}$ for respectively internal and secondary field amplitudes for a circular finitely conducting cylinder.

The resulting matrix equation is

$$\sum_{j=1}^{4} \mathrm{A}_{ij} x_j = \mathrm{b}_i\,, \quad i = 1,2,3,4\,, \tag{9}$$

for unknown coefficients

$$\begin{aligned}
x_1 &= \mathscr{E}_{nz}^{(s,q)}\,, \\
x_2 &= \mathscr{H}_{nz}^{(s,q)}\,, \\
x_3 &= \mathscr{E}_{nz}^{(i,q)}\,, \\
x_4 &= \mathscr{H}_{nz}^{(i,q)}\,,
\end{aligned} \tag{10}$$

where coefficient matrix is

$$\mathrm{A} = \begin{bmatrix}
H_n^{(1)}(\Omega_2) & 0 & -J_n(\Omega_1) & 0 \\
0 & H_n^{(1)}(\Omega_2) & 0 & -J_n(\Omega_1) \\
\frac{-nK}{\gamma_2^2 a} H_n^{(1)}(\Omega_2) & \frac{-i\omega\mu_0}{\gamma_2} H_n^{(1)\prime}(\Omega_2) & \frac{nK}{\gamma_1^2 a} J_n(\Omega_1) & \frac{i\omega\mu_0}{\gamma_1} J_n{}'(\Omega_1) \\
\frac{-\tilde{\sigma}_2}{\gamma_2} H_n^{(1)\prime}(\Omega_2) & \frac{-nK}{\gamma_2^2 a} H_n^{(1)}(\Omega_2) & \frac{\tilde{\sigma}_1}{\gamma_1} J_n{}'(\Omega_1) & \frac{nK}{\gamma_1^2 a} J_n(\Omega_1)
\end{bmatrix} \tag{11}$$

and for right-hand-side elements

$$\begin{aligned}
b_1 &= -\mathscr{E}_{nz}^{(0,q)} J_n(\Omega_2)\,, \\
b_2 &= -\mathscr{H}_{nz}^{(0,q)} J_n(\Omega_2)\,, \\
b_3 &= \tfrac{i\omega\mu_0}{\gamma_2} \mathscr{H}_{nz}^{(0,q)} J_n{}'(\Omega_2) + \tfrac{nK}{\gamma_2^2 a} \mathscr{E}_{nz}^{(0,q)} J_n(\Omega_2)\,, \\
b_4 &= \tfrac{nK}{\gamma_2^2 a} \mathscr{H}_{nz}^{(0,q)} J_n(\Omega_2) + \tfrac{\tilde{\sigma}_2}{\gamma_2} \mathscr{E}_{nz}^{(0,q)} J_n{}'(\Omega_2)\,.
\end{aligned} \tag{12}$$

The formal solution to matrix equation (9) for exterior field amplitudes is

$$\begin{aligned}
\mathscr{E}_{nz}^{(s,q)} &= \mathrm{N}_1/(\Delta \mathrm{A}_{24})\,, \\
\mathscr{H}_{nz}^{(s,q)} &= \mathrm{N}_2/(\Delta \mathrm{A}_{13})\,,
\end{aligned} \tag{13}$$

and

$$\begin{aligned}
\mathrm{N}_1 = {} & (\mathrm{A}_{24}\mathrm{A}_{42} - \mathrm{A}_{22}\mathrm{A}_{44})(\mathrm{b}_3\mathrm{A}_{13}\mathrm{A}_{24} - \mathrm{b}_1\mathrm{A}_{24}\mathrm{A}_{33} - \mathrm{b}_2\mathrm{A}_{13}\mathrm{A}_{34}) - \\
& (\mathrm{A}_{24}\mathrm{A}_{32} - \mathrm{A}_{22}\mathrm{A}_{34})(\mathrm{b}_4\mathrm{A}_{13}\mathrm{A}_{24} - \mathrm{b}_1\mathrm{A}_{24}\mathrm{A}_{43} - \mathrm{b}_2\mathrm{A}_{13}\mathrm{A}_{44})\,, \\
\mathrm{N}_2 = {} & (\mathrm{A}_{13}\mathrm{A}_{31} - \mathrm{A}_{11}\mathrm{A}_{33})(\mathrm{b}_4\mathrm{A}_{13}\mathrm{A}_{24} - \mathrm{b}_1\mathrm{A}_{24}\mathrm{A}_{43} - \mathrm{b}_2\mathrm{A}_{13}\mathrm{A}_{44}) - \\
& (\mathrm{A}_{13}\mathrm{A}_{41} - \mathrm{A}_{11}\mathrm{A}_{43})(\mathrm{b}_3\mathrm{A}_{13}\mathrm{A}_{24} - \mathrm{b}_1\mathrm{A}_{24}\mathrm{A}_{33} - \mathrm{b}_2\mathrm{A}_{13}\mathrm{A}_{34})\,,
\end{aligned} \tag{14}$$

where determinant $\Delta = \det(\mathrm{A})$ is

$$\begin{aligned}
\Delta = {} & (nKa)^2 (1/\Omega_2^2 - 1/\Omega_1^2)^2 J_n^2(\Omega_1) H_n^{(1)2}(\Omega_2) - \\
& \left(J_n(\Omega_1) H_n^{(1)\prime}(\Omega_2)/\Omega_2 - H_n^{(1)}(\Omega_2) J_n{}'(\Omega_1)/\Omega_1\right) \\
& \left(\Omega_2^2 J_n(\Omega_1) H_n^{(1)\prime}(\Omega_2)/\Omega_2 - (k_1 a)^2 H_n^{(1)}(\Omega_2) J_n{}'(\Omega_1)/\Omega_1\right),
\end{aligned} \tag{15}$$

and Bessel function arguments are defined as

$$\Omega_j = \gamma_j a\,, \quad j = 1,2\,. \tag{16}$$

The associated internal axial field coefficients for $\rho < a$ are

$$\begin{aligned}
\mathscr{E}_{nz}^{(i,q)} &= \left(\mathscr{E}_{nz}^{(0,q)} J_n(\Omega_2) + \mathscr{E}_{nz}^{(s,q)} H_n^{(1)}(\Omega_2)\right)/J_n(\Omega_1)\,, \\
\mathscr{H}_{nz}^{(i,q)} &= \left(\mathscr{H}_{nz}^{(0,q)} J_n(\Omega_2) + \mathscr{H}_{nz}^{(s,q)} H_n^{(1)}(\Omega_2)\right)/J_n(\Omega_1)\,.
\end{aligned} \tag{17}$$

Then, for example, from equation (1), the radial component of the electric field for a q directed dipole source is

$$\mathrm{E}_\rho^{(s,q)}(\rho,\phi,z) = \sum_{n=-\infty}^{\infty} e^{in\phi} \int_{-\infty}^{\infty} \mathscr{E}_{n\rho}^{(s,q)} J_n(\gamma_2\rho)\, e^{iKz}\, \frac{\mathrm{d}K}{2\pi}\,, \tag{18}$$

and similarly for all other components.

Numerical Results

The formulation of incident field representations of the form given for example by equation (18) are compared with their more simple rectangular coordinate closed form solutions. This checks both the algebra and the numerical algorithms used to evaluate the transforms for all six field components and three polarizations. All six components of $\mathbf{E}^{(0)}$ and $\mathbf{H}^{(0)}$ for the Cartesian and Fourier-Bessel expansions for a ϕ oriented electric dipole are compared, but here only $\mathrm{E}_\rho^{(0,\phi)}$ is displayed. The source frequency is 1 Hz as appropriate

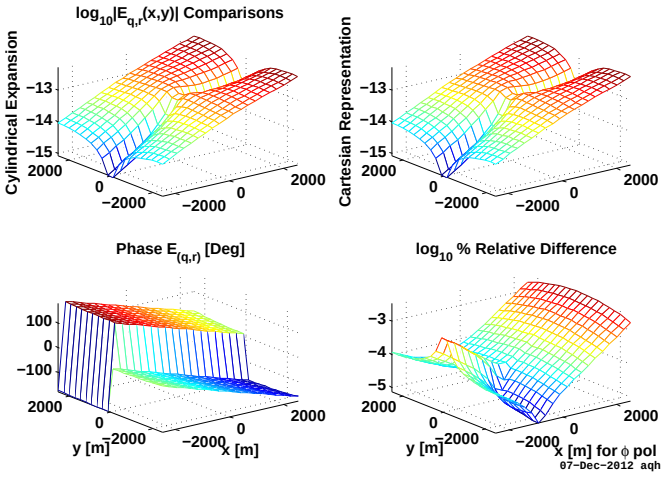

Figure 1: Magnitude and phase comparison of Cartesian and Fourier-Bessel series representations of $\mathrm{E}_{\rho}^{(0,\phi)}(x,y)$ for $z=0$.

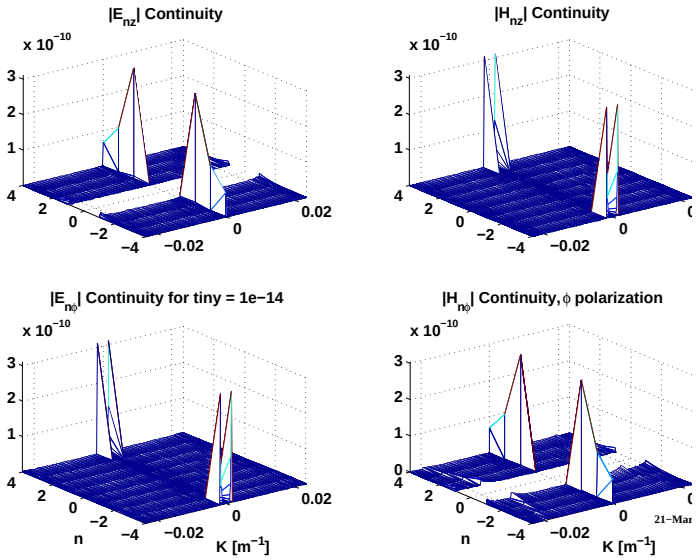

Figure 2: *Magnitude boundary condition verification for the four tangential field components at the cylinder interface as a function of the angular ordem n and z wavenumber K.*

for sea-bed logging, the background conductivity is 0.1 S/m,

and the dipole source amplitude is $I_0\,\mathrm{d}\ell = 1$ A. The source dipole is located at $\rho_T = 1.0\times10^4$ m, $\phi_T = 0$ radians, and $z_T = 0$ m. The observation point is $z=0$ with (x,y) as independent variables in the figures. Fourier transform uses a compound two 128 point real-axis Gauss-Legendre weights and abscissa integration with respectively finite intervals $[-\kappa,0]$ and $[0,\kappa]$ to more accurately track more rapid integrand variation for $|K| < \max(|k_1|,|k_2|)$. Upper limit κ is chosen such that the Hankel functions $H_n^{(1)}$ exponential factor has value $|e^{i\gamma\rho_{min}}| = 1.0\times10^{-8}$. Note that for this polarization the incident field components $\mathrm{E}_z^{(0,\phi)}, \mathrm{H}_{\rho}^{(0,\phi)}$ and

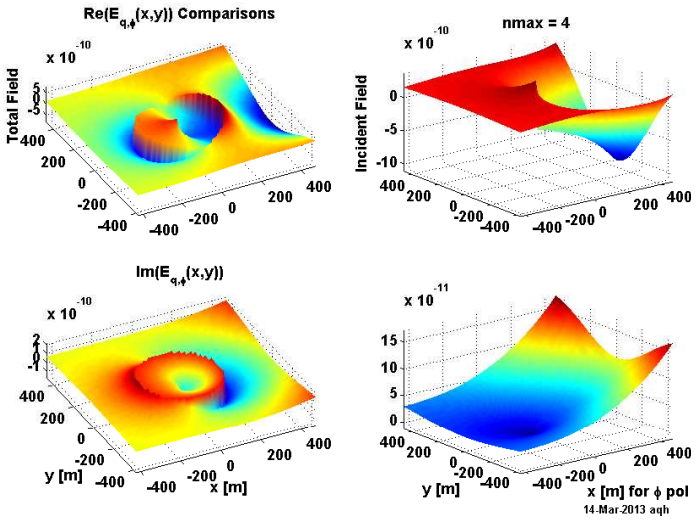

Figure 3: *Real and imaginary parts of total and incident components of E_{ϕ} as function of (x,y). Left-hand-side plots are total fields, right- hand- side are incident fields.*

$\mathrm{H}_{\phi}^{(0,\phi)}$ are correctly zero to machine precision. Similar accuracy is observed but not plotted for the remaining six field components for the ρ and z polarizations.

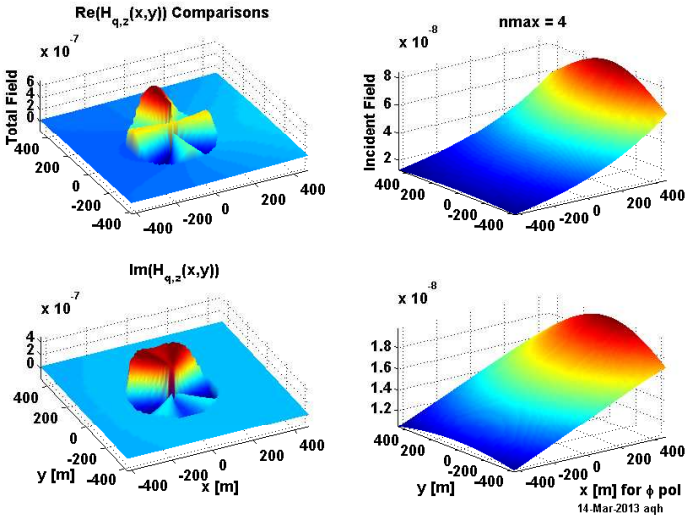

Figure 4: *Real and imaginary parts of total and incident components of H_z as function of (x,y). Left-hand-side plots are total fields, right- hand- side are incident fields.*

The four by four matrix equation (9) is ill-conditioned prompting the use of truncated singular value decomposition (TSVD) (Golub, 1989) rather than Cramer's rule analytical result as given by equation (14). The TSVD trucation parameter here is $\mathrm{tiny} = 1.0\times10^{-14}$. The four sub-plot dependent functions are of the normalized form $(|\mathrm{left-hand-side})/\mathrm{right-hand-side}) - 1|$. The plots show between 9 and 12 figure agreement with the greatest errors typically where magnitudes of n is large and K is small.

Here, for lack of space, only two components of the total fields are displayed. Fig. 3 plots the real and imaginary parts of total and incident components of E_ϕ as a function of (x,y). The presence of the cylinder is prominent. Fig. 4 plots the real and imaginary parts of the total and incident components of H_z as a function of (x,y). This component shows complicated angular field structure inside the cylinder prompting the use of a Lanczos filter (Hamming, 1983). Comparison of the real and imaginary parts of the total field component H_z displays the expected $e^{in\phi}$ behavior : relative maxima of the real part corresponds to relative minima of the imaginary part. For this ρ directed dipole, the field components E_z, H_ρ and H_ϕ are not excited and as in the case of the incident field comparisons are computed to be machine zero.

Conclusions and Recommendations

This report gives a concise angular harmonic development of vector electromagnetic field scattering from a permeable and conducting cylinder for all possible orientations of an electric dipole source. The motivation here is to have an analytic model for a finite cross section anomaly with which to compare more general vector field finite-difference frequency domain solvers. In common with fiber optical waveguide formulations, all fields are represented in terms of the axial components $(\mathrm{E}_z, \mathrm{H}_z)$. Matching boundary conditions in the transform domain for each angular index n and Fourier transform variable K leads a set of possibly ill-conditioned 4x4 matrices. The solutions to these equations are validated numerically. Solution of the matrix equations use TSVD. All six components of the Fourier- Bessel expansions for incident field, and for each of the three independent polarizations are validated numerically by comparisons with their analogous rectangular coordinate closed form representations.

A possible relatively straight-forward modification is to extend the results for internal dipole sources. Depending on the orientation and location of the so synthesized extended source, integrate the electric dipole components around a closed loop inside the cylinder, and then compute the resulting magnetic flux at a receiver loop. This model then can compute the exact borehole fields for tri-axial induction arrays as now used in the well logging industry. Such results could then be used for environmental borehole and standoff corrections. In addition, the results could be used to check the accuracy of the commonly used magnetic dipole approximations.

References

Papas, C. H., 1950, Diffraction by a cylindrical obstacle, J. Appl. Physics, vol. 21, p318-325

Wait, J. R. , 1959, Electromagnetic Radiation from Cylindrical Structures, Pergamon Press Inc., New York

Tai, C. T., 1971, Dyadic Green's Functions in Electromagnetic Theory, Intext Educational Publishers, Scranton

Okamoto, K., 2006, Fundamentals of Optical Waveguides, Sec. Ed., Academic Press, Burlington, MA. p58-59

Tsandoulas, G. N., 1968, Scattering of a Dipole Field by Finitely Conducting and Dielectric Circular Cylinders, IEEE Trans. Ant. and Prop., vol. 16, p324-328

A. Illahi, A., and Q. A. Naqvi and K. Hongo, 2008, Scattering of Dipole Field by a finite conducting and a finite impedance cylinder, Progress in Electromagnetic Research M, vol. 1, p139-184

Hamming, R. W. , 1983, Digital Filters, Second Edition, Prentice-Hall, Inc., Englewood Cliffs, NJ, p93-101

Golub G. H. and C. F. Van Loan, 1989, Matrix Computations, Sec. Edition, John Hopkins Series in Mathematical Sciences

Acknowledgments

I wish to thank my colleagues Professors Cicero Roberto Teixeira Rêgis, Marcos Welby Corrêa da Silva and João Batista Corrêa da Silva at the INSTITUTO DE GEOCIÊNCIAS, FACULDADE DE GEOFÍSICA, Universidade do Pará for their efforts in facilitating this opportunity to again participate in geophysical research and teaching in Brazil.